Article

Discovery Medicine 2024; 36(184): 923–935
https://doi.org/10.24976/Discov.Med.202436184.86

Regulation of the *RB1* Gene through DNMT1 by SGI-1027 and its Impact on the Growth and Metastasis of Gastric Cancer Cells

Peixing Gu[1], Wenjie Huang[1], Wentian Lu[1], Peng Shu[1,*]

[1]Department of Medical Oncology, Affiliated Hospital of Nanjing University of Chinese Medicine, 210004 Nanjing, Jiangsu, China
*Correspondence: 18652962586@163.com (Peng Shu)
Published: 20 May 2024

Background: SGI-1027 is a recognized inhibitor of DNA methyltransferase 1 (DNMT1), and earlier investigations have indicated an inverse correlation between dysregulated DNMT1 expression in gastric cancer (GC) and retinoblastoma 1 (*RB1*) gene expression. Despite this knowledge, the precise mechanisms underlying the action of SGI-1027 in GC cells remain inadequately comprehended. The primary objective of this study is to elucidate the impact of SGI-1027 on the behavior of GC cells, encompassing aspects such as growth and metastatic potential, by intervening in DNMT1, thereby influencing the regulation of *RB1* gene expression.

Method: The acquisition of the normal gastric mucosal cell line GES-1 and the human gastric cancer cell line MKN45 was followed by employing Western blot (WB) and quantitative reverse transcription-polymerase chain reaction (qRT-PCR) techniques to evaluate the expression levels of RB1 and DNMT1 in these two cell lines. Subsequently, the MKN45 cell line was cultured in medium containing varying concentrations of SGI-1027, and the impact of SGI-1027 on the regulation of *RB1* and DNMT1 in GC cells was reassessed using WB and qRT-PCR techniques. To scrutinize the effect of SGI-1027 on GC cells, we utilized the 3-(4,5-dimethyl-2-thiazolyl)-2,5-diphenyl-2H tetrazolium bromide (MTT) assay to determine cell proliferation and performed Transwell experiments to assess cell migration and invasion capabilities. Throughout this process, we also employed WB to assess the levels of cell cycle-associated proteins (Cyclin D1, Cyclin E1, and Cyclin B1) and proteins related to apoptosis (BCL-2 associated protein X apoptosis regulator (BAX) and B-cell lymphoma 2 apoptosis regulator (BCL-2)). Furthermore, we injected the MKN45 cell line and MKN45 cell line cultured with the optimal concentration of SGI-1027 for 5 days and 10 days into mice subcutaneously and through the tail vein, dividing them into the Model group, Model+SGI-1027 5d group, and Model+SGI-1027 10d group. We monitored changes in tumor size and volume in mice, and tumor tissues as well as lung tissues were collected for hematoxylin and eosin (HE) staining. Finally, DNMT1 expression levels in GC tissues were detected using both WB and immunohistochemistry (IHC) techniques. Additionally, RB1 expression levels in GC tissues were assessed using WB.

Result: In contrast to GES-1 cells, MKN45 cells displayed a distinctive profile characterized by increased DNMT1 expression and decreased RB1 expression ($p < 0.05$). However, upon the introduction of SGI-1027, a notable decrease in DNMT1 levels within GC cells was observed, concomitant with an elevation in *RB1* gene expression, with 25 µmol/L SGI-1027 identified as the optimal concentration ($p < 0.05$). Functional assays demonstrated that SGI-1027-treated GC cells exhibited pronounced features of inhibited proliferation, migration, and invasion when compared to untreated MKN45 cells ($p < 0.05$). Moreover, in SGI-1027-treated GC cells, the levels of Cyclin D1, Cyclin E1, Cyclin B1, and BCL-2 were significantly reduced, while the expression level of BAX increased ($p < 0.05$). Notably, the most pronounced impact was observed at 25 µmol/L SGI-1027, further underscoring its regulatory effects on tumor cell behavior ($p < 0.05$). In animal experiments, the Model group exhibited a substantial increase in tumor volume, with HE staining results indicating extensive necrosis in most gastric tissues and noticeable signs of lung metastasis, accompanied by increased DNMT1 expression and decreased *RB1* gene expression. In contrast, the SGI-1027 group displayed a reduction in gastric tumor volume, decreased necrosis, and reduced lung tumor metastasis ($p < 0.05$). Additionally, the expression of DNMT1 was significantly reduced in SGI-1027-treated GC cells, while RB1 expression increased ($p < 0.05$), further confirming the inhibitory effects of SGI-1027 on tumor growth and metastasis.

Conclusions: SGI-1027 effectively hinders the proliferation and dissemination of GC cells by downregulating DNMT1 and promoting the expression of *RB1*.

Keywords: SGI-1027; DNMT1; *RB1* gene; gastric cancer

Introduction

Gastric cancer (GC) is a malignancy originating from the epithelial cells of the stomach, which line the interior and play a crucial role in secreting gastric acid and digestive juices for food digestion. Given its position in the digestive system, the stomach is regularly exposed to food and potential carcinogens, increasing the likelihood of genetic mutations or damage in epithelial cells. This, in turn, can lead to the transformation of normal cells into malignant cancer cells [1,2].

Adenocarcinoma represents the predominant histopathological pattern of GC, typically arising from the innermost lining of the stomach's mucosa—the shallowest layer of the stomach wall [3,4]. However, as the disease advances, adenocarcinoma may progressively infiltrate deeper layers of tissue. Once cancer extends to deeper tissues, the challenges associated with treatment intensify [5–7]. Therefore, the timely detection and intervention are pivotal for improving the chances of a successful therapeutic outcome.

DNA methyltransferase 1 (DNMT1) plays a pivotal role in regulating gene expression by engaging with protein complexes to either maintain the silence or activate genes [8,9]. Anomalies in DNMT1 activity or expression levels are intricately linked to various diseases, with a particular emphasis on cancer [10,11]. In cancer, DNMT1 is frequently overexpressed, leading to the overactivation of oncogenes and the inactivation of tumor suppressor genes [12,13]. This abnormal DNMT1 activity significantly influences gene expression and function, fostering tumor development [14,15].

Aberrant changes in oncogenes, which typically govern normal cell growth and differentiation, result in their activation, propelling uncontrolled proliferation of cancer cells. Such activated oncogenes contribute to abnormal cell growth and malignant transformation [16,17]. Conversely, tumor suppressor genes are often suppressed or inactivated, depriving them of their role in inhibiting the proliferation of cancer cells. This allows cancer cells to evade normal cellular growth regulation [18,19].

Research indicates a substantial increase in DNMT1 expression levels in tissue samples from many GC patients. Elevated levels of DNMT1 expression closely correlate with the initiation and progression of GC.

RB1, also recognized as the "retinoblastoma 1" gene, is a crucial tumor suppressor gene encoding the Retinoblastoma protein (RB protein) that plays an essential role in maintaining normal cell growth and controlling the cell cycle [20,21]. In certain cancers, the *RB1* gene may undergo regulatory disruptions, often involving direct interaction with DNMT1 [22,23]. This interaction prompts transcription factors to bind to the regulatory or promoter region of the *RB1* gene, leading to a reduction in its normal transcription [24,25]. Suppression of *RB1* gene expression results in the loss of normal cell cycle control, leading to the overexpression of cell cycle proteins and a decrease in the expression of apoptosis-related proteins. This makes cancer cells more prone to survival and proliferation [26]. Normally, *RB1* governs the progression of the cell cycle by inhibiting the function of cyclin-dependent kinases [27,28]. Inactive or mutated *RB1* genes can lead to a lack of proper control over proliferation, facilitating cancer progression [29].

Beyond cell cycle control, *RB1*'s role extends to processes such as cell migration and invasion [30]. Inactivation of *RB1* may render cancer cells more prone to migrating and invading surrounding tissues, while normal *RB1* function helps maintain cellular stability, promotes apoptosis, and thereby prevents cancer development [31]. In cancers like GC, the coexistence of high DNMT1 expression and *RB1* inactivation is common. Elevated DNMT1 levels may silence the *RB1* gene, diminishing the expression of the RB1 protein. As the RB1 protein crucially regulates the cell cycle, its inactivation leads to uncontrolled cell proliferation, bypassing normal cycle control, and favoring the growth and spread of cancer cells [32].

SGI-1027, as a DNA methyltransferase 1 (DNMT1) inhibitor, effectively diminishes the activity of DNMT enzymes, facilitating the restoration of normal function to the *RB1* gene [33,34]. This critical process is instrumental in curbing the abnormal proliferation of GC cells and mitigating their propensity to metastasize. The utilization of SGI-1027 shows promise in restricting cancer spread and growth, positioning it as a valuable component in therapeutic strategies aimed at decelerating cancer progression. This approach reveals new directions and instills hope for potential advancements in cancer treatments.

Materials and Methods

Preparation of SGI-1027 Solution

A 50 mmol/L stock solution of SGI-1027 from Selleck Chemicals, Houston, TX, USA, was prepared using dimethyl sulfoxide (DMSO). Subsequently, drug administration solutions of 15 µmol/L, 20 µmol/L, and 25 µmol/L were prepared in the medium. These solutions were used as controls in a medium containing 0.1% DMSO. The stock solution is stored at –20 °C for an extended period.

Cell Culture

The human gastric mucosal epithelial cell line GES-1 and the human gastric cancer cell line MKN45 cells were procured from Procell Life Science & Technology (Wuhan, China). These cell lines were cultured separately in RPMI-1640 medium (Invitrogen) supplemented with 10% fetal bovine serum (FBS). Subsequently, MKN45 cells were subjected to treatment with SGI-1027, dissolved in DMSO, at various concentrations (15 µmol/L, 20 µmol/L, 25 µmol/L, with 0.1% DMSO as the control). The culture conditions were maintained at 37 °C, 5% CO_2, and high humidity. Before the experiment, all cells underwent short tandem repeat (STR) identification and mycoplasma testing, ensuring that STR identification of all cell lines was consistent with reference values in the database and that no signs of mycoplasma infection were detected. All procedures adhere to aseptic techniques to prevent cell contamination.

Western Blot

Protein extraction was performed using Radio Immunoprecipitation Assay (RIPA) lysis solution (P0013B, Beyotime, Shanghai, China). Following quantification with a bicinchoninic acid (BCA) Kit (P0012, Beyotime, Shanghai, China), the proteins were subjected to SDS-PAGE electrophoresis and subsequently transferred onto a polyvinylidene fluoride (PVDF) membrane. The PVDF membrane was immersed in 5% skim milk for 2 hours to prevent nonspecific binding.

Subsequently, the PVDF membrane was incubated with primary antibodies against RB1 (1:1000, ab184796, Abcam, Cambridge, MA, USA), DNMT1 (1:1000, ab134148, Abcam, Cambridge, UK), Cyclin D1 (1:1000, ab226977, Abcam), Cyclin E1 (1:1000, ab13266, Abcam), and Cyclin B1 (1:1000, ab13439, Abcam) overnight at 4 °C. Following this, the membrane was exposed to secondary antibodies (1:2000, ab6721, Abcam) for 1 hour under ambient conditions to facilitate binding with the primary antibodies. The internal control used was Glyceraldehyde-3-phosphate dehydrogenase (GAPDH) (1:1000, ab8245, Abcam).

Finally, an enhanced chemiluminescence kit was employed to visualize protein signals, and relative protein expression analysis was carried out using ImageJ software (V1.8.0.112, NIH, Madison, WI, USA).

qRT-PCR

RNA isolation from cells and tissues was conducted using TRIzol solution (Invitrogen). Subsequently, cDNA was synthesized using the PrimeScript RT kit (Takara, Dalian, China). The synthesized cDNA was then combined with specific primers, and PCR amplifications were performed in a PCR system using SYBR Premix Ex TaqII (TaKaRa, Otsu City, Japan). The results were recorded using ABI StepOne™ Software v2.3 (Applied Biosystems, Foster City, CA, USA).

In this process, the $2^{-\Delta\Delta Ct}$ method was employed to calculate the expression levels of *RB1* and *DNMT1*, with *GAPDH* serving as an internal reference. The primer sequence is shown in Table 1.

MTT Assay

Cells were seeded into 96-well plates at a density of 4×10^3 cells per well. Subsequently, 25 µL of 3-(4,5-dimethyl-2-thiazolyl)-2,5-diphenyl-2H tetrazolium bromide (MTT) solution (Sigma, St. Louis, MO, USA) was added to each well, and the plate was placed in a CO_2 incubator at 37 °C. Finally, the optical density at 490 nm was measured using a microplate reader (Biotek, Winooski, VT, USA).

Transwell

Transwell assays were employed to assess the migratory and invasive capabilities of the cells. The bottom chamber was filled with 600 µL of medium enriched with 20% FBS, while the top chamber was layered with 200 µL of Dulbecco's modified Eagle's medium (DMEM) without serum. To evaluate the cells' invasive capacity, the upper chamber was supplemented with Matrigel (BD Bioscience, Franklin Lake, NJ, USA) at a concentration of 2 mg/mL.

Cells were seeded in the upper chamber at a density of 5×10^4 cells/mL and subsequently incubated at 37 °C with 5% CO_2 for 24 hours. Following incubation, the cells in the bottom chamber were fixed with 4% Paraformaldehyde (PFA) and then stained with 0.01% crystal violet (Servicebio Technology Co., Ltd., Wuhan, China). Ultimately, the stained cells were counted using a microscope (DP74; Olympus Corporation, Tokyo, Japan).

Animal Experiment

All animal trials strictly adhered to the "Laboratory Animal Care and Use Guidelines" and received approval from the Ethics Committee of Affiliated Hospital of Nanjing University of Chinese Medicine (Lot Number: 202104008). Male BALB/c nude mice (Slack, Jingda, Changsha, China), aged between 4–6 weeks and weighing 18–20 g, were procured and maintained in a pathogen-free environment.

MKN45 cells and MKN45 cells cultured in 25 µmol/L SGI-1027 medium for 5 days and 10 days were subcutaneously injected into BALB/c nude mice at a concentration of 1×10^7 cells/200 µL and administered through caudal vein injection, respectively. The mice were categorized into the following groups: Model, Model+5d 25 µmol/L SGI-1027, Model+10d 25 µmol/L SGI-1027. The growth of the transplanted tumor was monitored every 4 days, and the dimensions and mass of the tumor were documented. After 4 weeks, the mice were euthanized under 2%–3% isoflurane anesthesia via cervical dislocation, and both tumor tissue and lung tissue were harvested for further analysis. The tumor volume (V) is calculated according to the following formula: $V = \text{length} / 2 \times \text{width}^2$.

HE Staining

The tumor tissue samples were immersed in a 10% formalin solution and underwent ethanol gradient dehydration. Subsequently, these samples were encased in paraffin before being sectioned into 4 µm thick slices. The sections were then stained with hematoxylin and eosin (HE) (Sigma Aldrich, St. Louis, MO, USA). Finally, the stained sections were observed under an optical microscope (Leica Microsystems, Wetzlar, Germany).

Table 1. Primer sequences of *RB1* and *DNMT1*.

Human gene	F (5′-3′)	R (5′-3′)
DNMT1	TTGATGCGGAAACCCTGGAA	CGTGAAACATCTGCCCGTTG
RB1	AAGGACCGAGAAGGACCAAC	AAGGCTGAGGTTGCTTGTGT
GAPDH	GCAAATTCCATGGCACCGTC	AGCATCGCCCCACTTGATTT
Mouse gene	F (5′-3′)	R (5′-3′)
RB1	GAGCTTGGCTAACTTGGGAGA	AGTGCAGGAGGTGAGAACTTA
GAPDH	GTGAACGGATTTGGCCGTATTG	GCAACAATCTCCACTTTGCCACT

DNMT1, DNA methyltransferase 1; *RB1*, retinoblastoma 1; *GAPDH*, Glyceraldehyde-3-phosphate dehydrogenase.

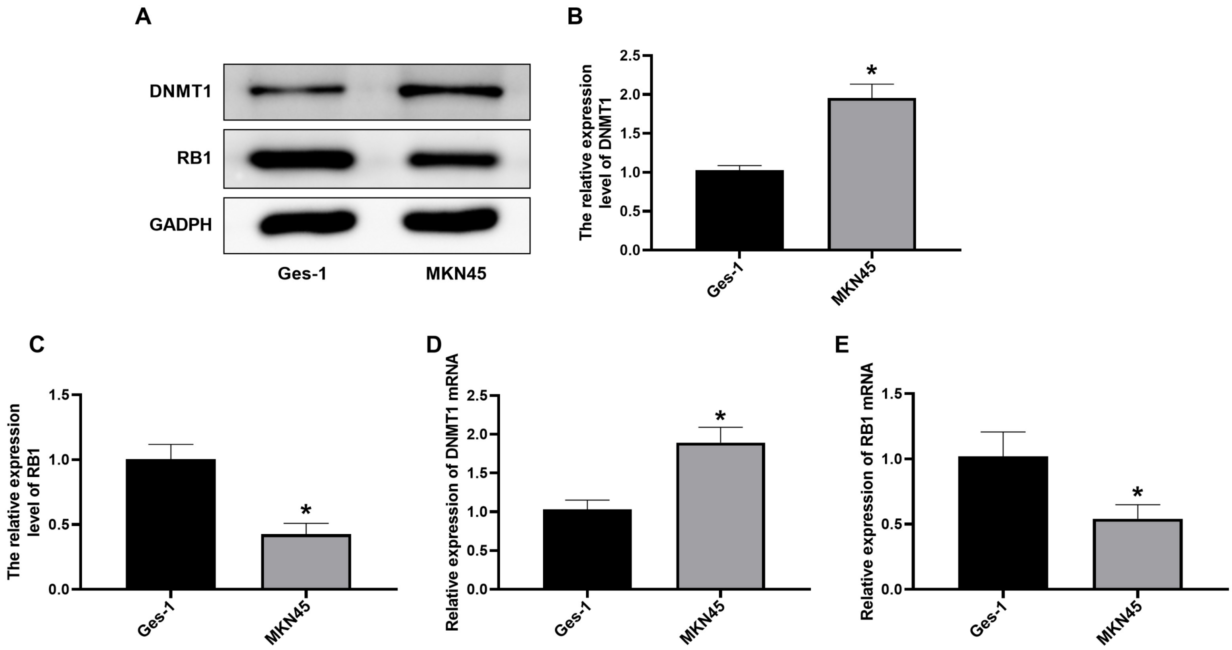

Fig. 1. Expression of *RB1* gene and DNMT1 in gastric cancer cells. (A–E) Detection of DNMT1 and RB1 expression by WB and qRT-PCR (n = 3). **p* < 0.05 versus the GES-1 group. WB, Western blot; qRT-PCR, quantitative reverse transcription-polymerase chain reaction.

Immunohistochemistry

The tumor tissue underwent fixation using 4% PFA, followed by paraffin embedding. Subsequently, tissue sections measuring 4 µm in thickness were prepared, and these sections were incubated with the primary antibody DNMT1 (1:1000, ab188453, Abcam). Following that, the tissue sections were subjected to incubation with a secondary goat anti-rabbit antibody for 2 hours at room temperature. Next, staining was performed using the Diamindbenzidine (DAB) staining kit (ZY6SK2020, Zeye-BIO, Shanghai, China) with a brief hematoxylin counterstaining for 30 seconds. Finally, the sections were examined under a microscope (Nikon, Tokyo, Japan).

Statistical Analysis

The experimental data were subjected to statistical analysis using GraphPad Prism 9 (Dotmatics, Boston, MA, USA). The data are presented as mean ± SD. Statistical differences among various groups were assessed through Student's *t*-test and Analysis of Variance (ANOVA) analysis. A significance level of $p < 0.05$ was considered statistically significant.

Results

DNMT1 Activity and RB1 Gene Expression in Gastric Cancer Cells

According to the results obtained from Western blot (WB) and quantitative reverse transcription-polymerase chain reaction (qRT-PCR), it was observed that the activity of DNMT1 in the human gastric cancer cell line MKN45 significantly increased compared to normal gastric mucosal epithelial cells GES-1, while the expression level of the *RB1* gene notably decreased ($p < 0.05$) (Fig. 1A–E).

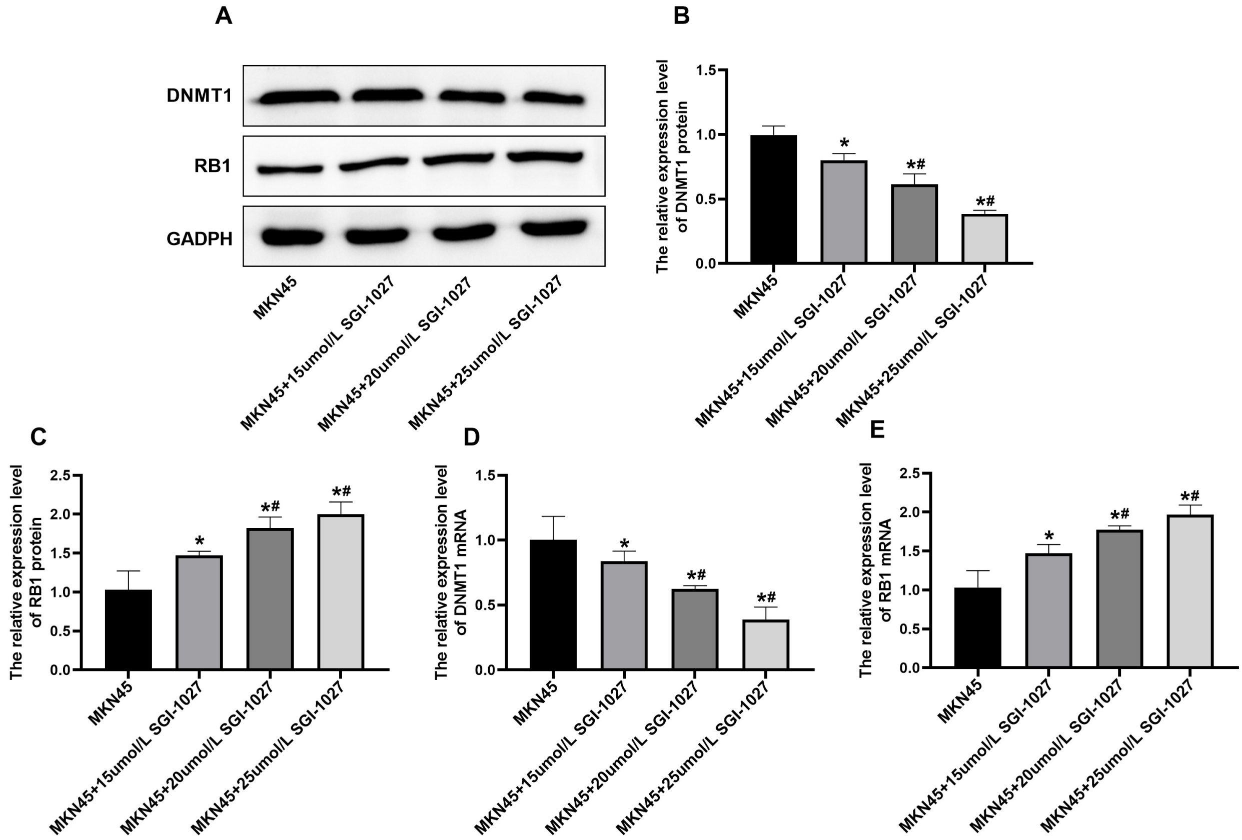

Fig. 2. Effect of SGI-1027 on expression of DNMT1 and RB1 in MKN45 cells. (A–E) Detection of DNMT1 and RB1 expression by WB and qRT-PCR (n = 3). *$p < 0.05$ versus the MKN45 group, #$p < 0.05$ versus the 15 µmol/L SGI-1027 group.

Impact of SGI-1027 on DNMT1 Activity and RB1 Gene Expression Level in GC Cells

The results clearly demonstrate a gradual decrease in the expression of DNMT1 and an increase in the content of the *RB1* gene in the SGI-1027 treatment groups at different concentrations (including 15 µmol/L, 20 µmol/L, and 25 µmol/L) when compared to the MKN45 group ($p < 0.05$). Furthermore, compared with the 15 µmol/L SGI-1027 group, there was a significant reduction in DNMT1 expression and an increase in *RB1* gene content in the 20 µmol/L and 25 µmol/L SGI-1027 groups ($p < 0.05$). Notably, these changes are most prominent in the 25 µmol/L SGI-1027 treatment group ($p < 0.05$) (Fig. 2A–E).

Impact of SGI-1027 on the Behavior of GC Cells through the DNMT1-RB1 Pathway

The results from the MTT and Transwell experiments demonstrate that, in comparison to the MKN45 group, SGI-1027 treatment at different concentrations (including 15 µmol/L, 20 µmol/L, and 25 µmol/L) exhibits significant inhibitory effects on cell proliferation, migration, and invasion abilities ($p < 0.05$). Furthermore, in comparison to the 15 µmol/L SGI-1027 group, cell proliferation, migration, and invasion were notably inhibited in the 20 µmol/L and 25 µmol/L SGI-1027 groups ($p < 0.05$). It is particularly noteworthy that these inhibitory effects on cell behavior are most pronounced in the 25 µmol/L SGI-1027 treatment group ($p < 0.05$) (Fig. 3A–C).

Impact of SGI-1027 on the Expression of Cell Cycle and Apoptotic Proteins in GC Cells through the DNMT1-RB1 Pathway

The WB results reveal that, in the SGI-1027 treatment groups at different concentrations (including 15 µmol/L, 20 µmol/L, and 25 µmol/L), the expression levels of cell cycle proteins (Cyclin D1, Cyclin E1, Cyclin B1) significantly decreased compared to the MKN45 group. Additionally, there was a marked reduction in the expression level of the anti-apoptotic protein B-cell lymphoma 2 apoptosis regulator (BCL-2), and correspondingly, an increase in the levels of the pro-apoptotic protein BCL-2 associated protein X apoptosis regulator (BAX) was observed ($p < 0.05$). Furthermore, when compared with the 15 µmol/L SGI-1027 group, the levels of cyclin and anti-apoptotic protein in the 20 µmol/L and 25 µmol/L SGI-1027 groups significantly decreased ($p < 0.05$). Notably, these changes are most pronounced in the 25 µmol/L SGI-1027 treatment group ($p < 0.05$) (Fig. 4A–G).

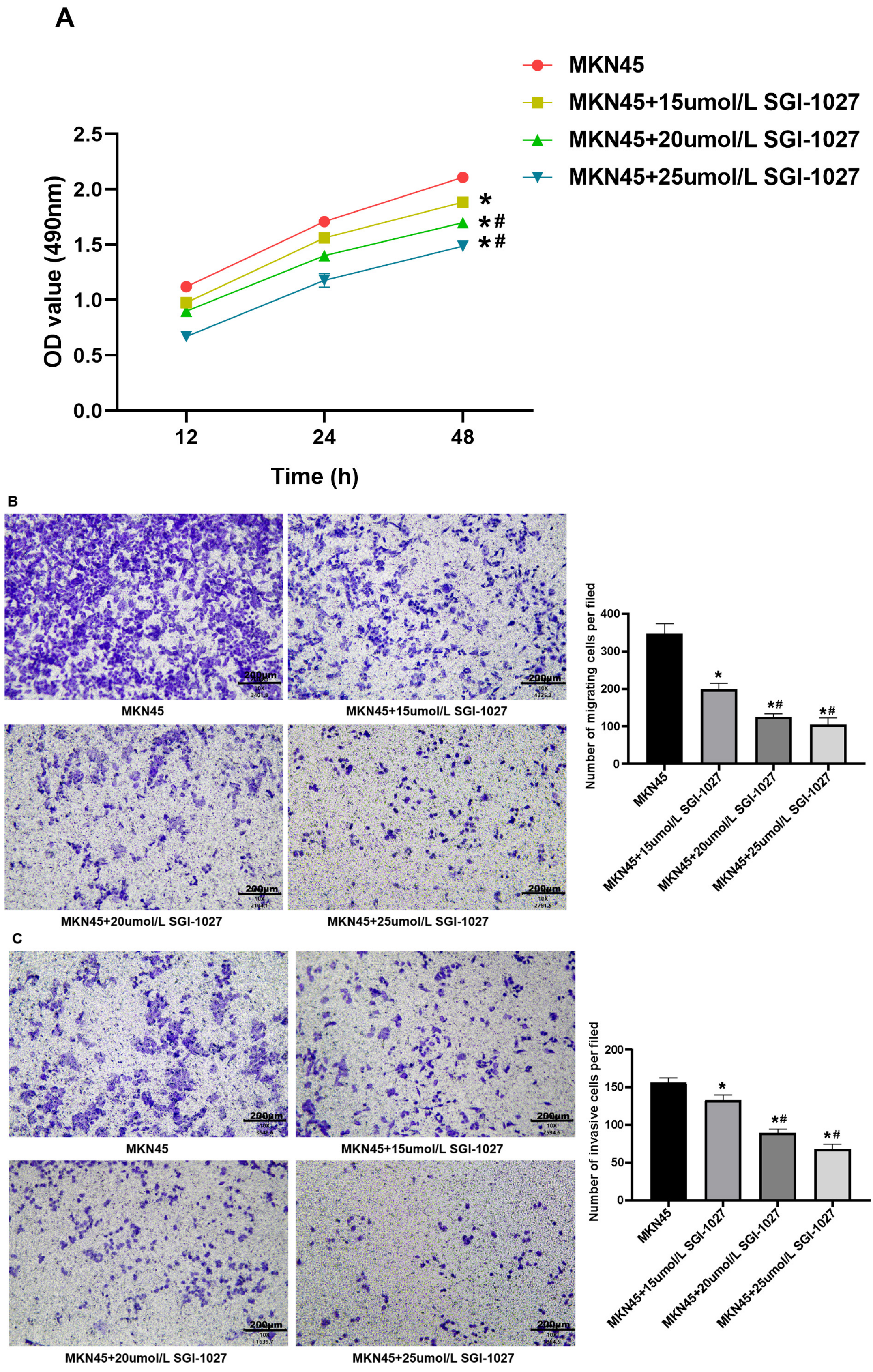

Fig. 3. Effect of SGI-1027 on growth and metastasis of MKN45 cells. (A) MTT detection of cell proliferation (n = 3). (B) Transwell detects cell migration. (C) Transwell detects cell invasion (n = 3). **p* < 0.05 versus the MKN45 group, #*p* < 0.05 versus the 15 µmol/L SGI-1027 group. OD, optical density; MTT, 3-(4,5-dimethyl-2-thiazolyl)-2,5-diphenyl-2H tetrazolium bromide.

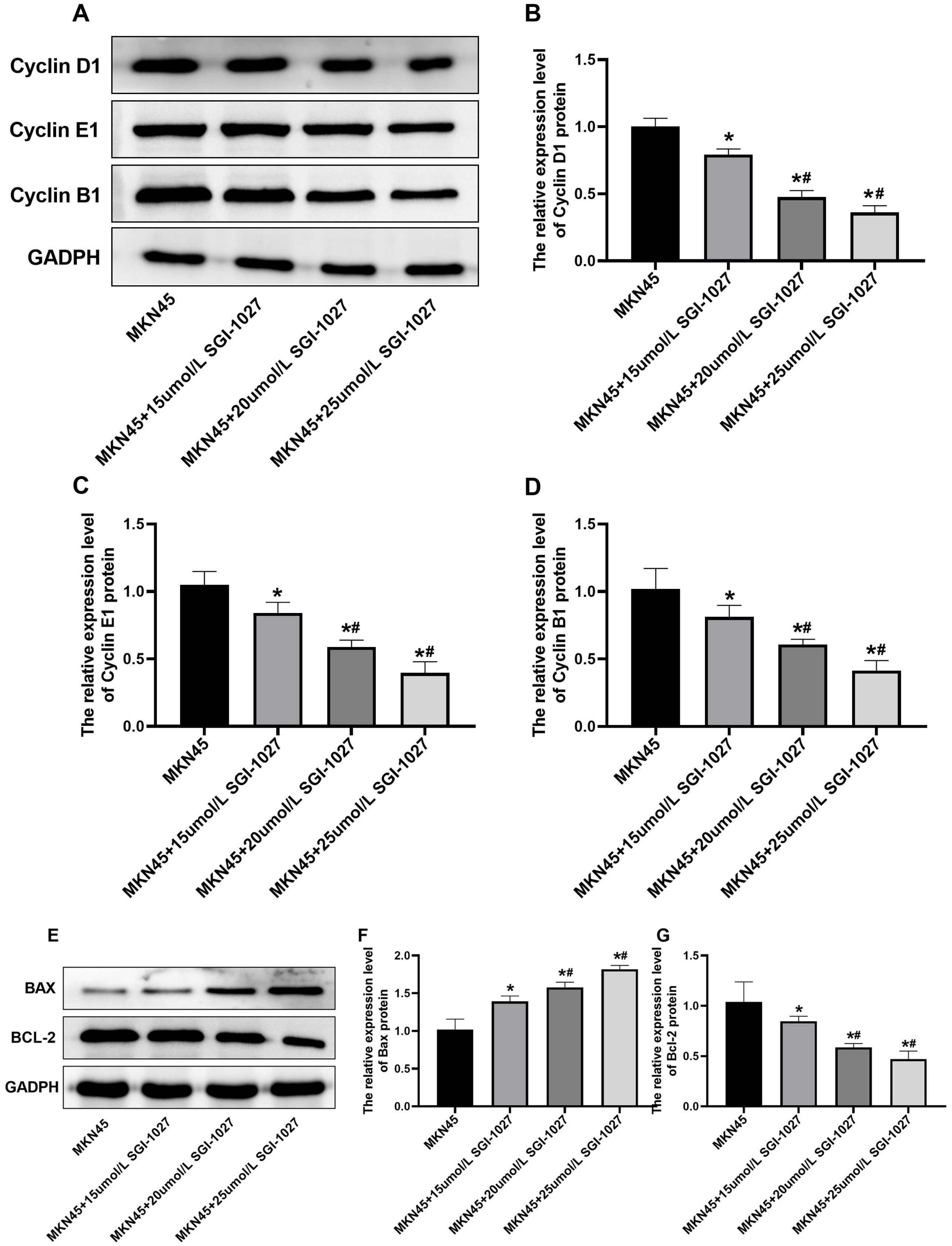

Fig. 4. Effects of SGI-1027 on cycle and apoptosis proteins in MKN45 cells. (A–G) Expression levels of cyclin and apoptotic proteins were measured by WB (n = 3). $^{*}p < 0.05$ versus the MKN45 group, $^{\#}p < 0.05$ versus the 15 μmol/L SGI-1027 group. BAX, BCL-2 associated protein X apoptosis regulator; BCL-2, B-cell lymphoma 2 apoptosis regulator.

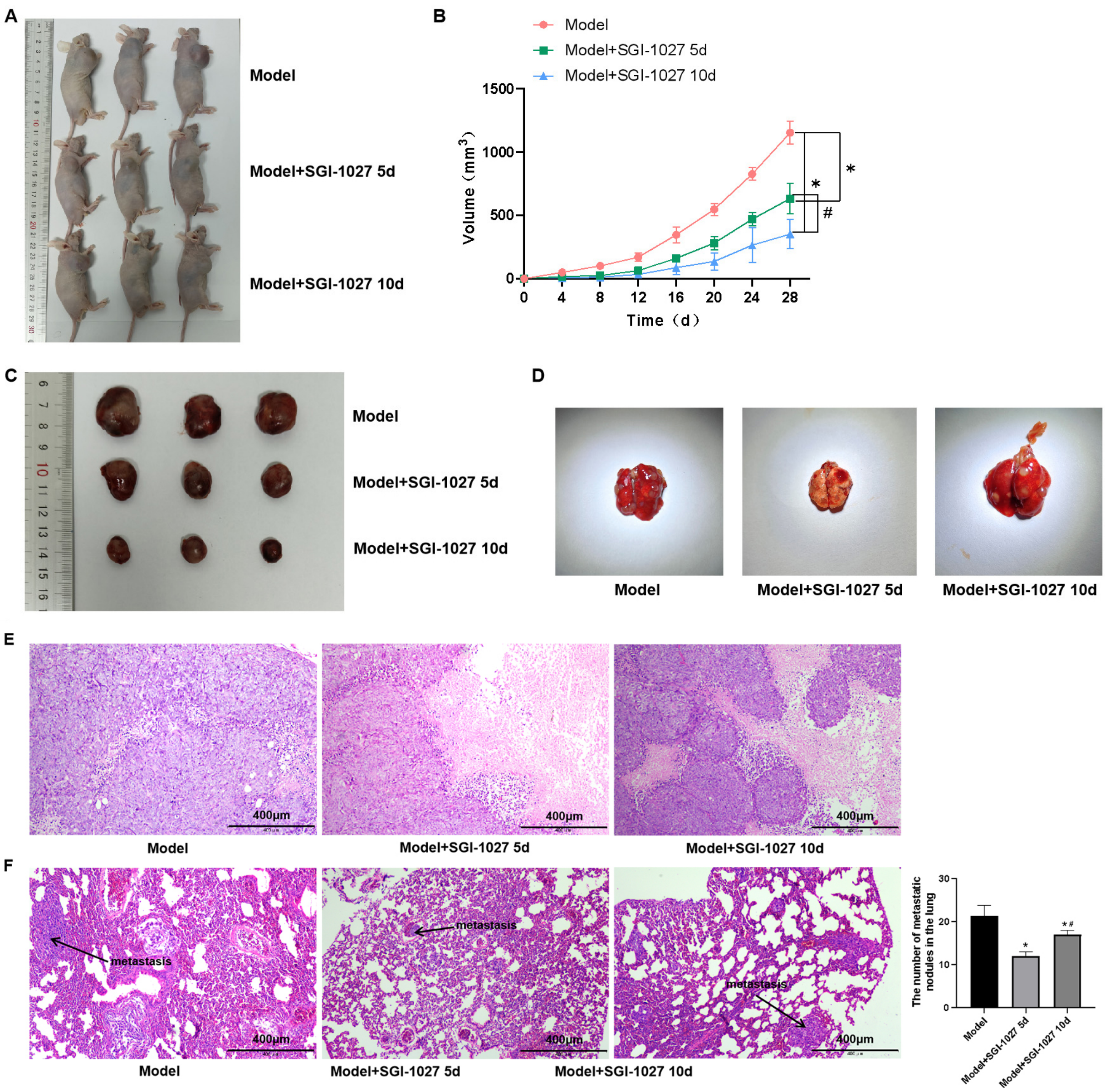

Fig. 5. Effects of SGI-1027 on growth and transfer in mice. (A–C) Changes in tumor size and volume. (D) Tumor lung metastasis (n = 3). (E) HE staining of the gastric tissue. (F) HE staining of the lung tissue (n = 3). *$p < 0.05$ versus the Model group, $^{\#}p < 0.05$ versus the Model+SGI-1027 5d group. HE, hematoxylin and eosin.

The Impact of SGI-1027 on the Growth and Metastasis of GC Tissue through the DNMT1-RB1 Pathway

The Nude Mice Tumor Formation and Metastasis Model were established by injecting MKN45 cells co-cultured with SGI-1027 for 5 and 10 days into nude mice to observe tumor growth. *In vivo* experimental results indicate that, in comparison to the Model group, tumor growth in the Model+SGI-1027 5d group and Model+SGI-1027 10d group was inhibited, leading to a reduction in tumor size and volume. Additionally, there was a decrease in the size and number of nodules in lung tissue, accompanied by a diminished degree of lung metastasis (Fig. 5A–D) ($p < 0.05$).

HE staining revealed distinctive features in the gastric tumors of the Model group, including irregular cell nuclei, inconspicuous nucleoli, a high nuclear-cytoplasmic ratio, and a small number of mitotic phenomena. In contrast, tumor tissues from the Model+SGI-1027 5d group and Model+SGI-1027 10d group exhibited fewer tumor cells, smaller and condensed nuclei, fragmentation, dissolution, and deeper staining (Fig. 5E).

Furthermore, compared to the Model group, lung tissues from the Model+SGI-1027 5d group and Model+SGI-1027 10d group displayed a reduced size and number of nodules, indicating a decrease in the extent of lung metastasis (Fig. 5F) ($p < 0.05$).

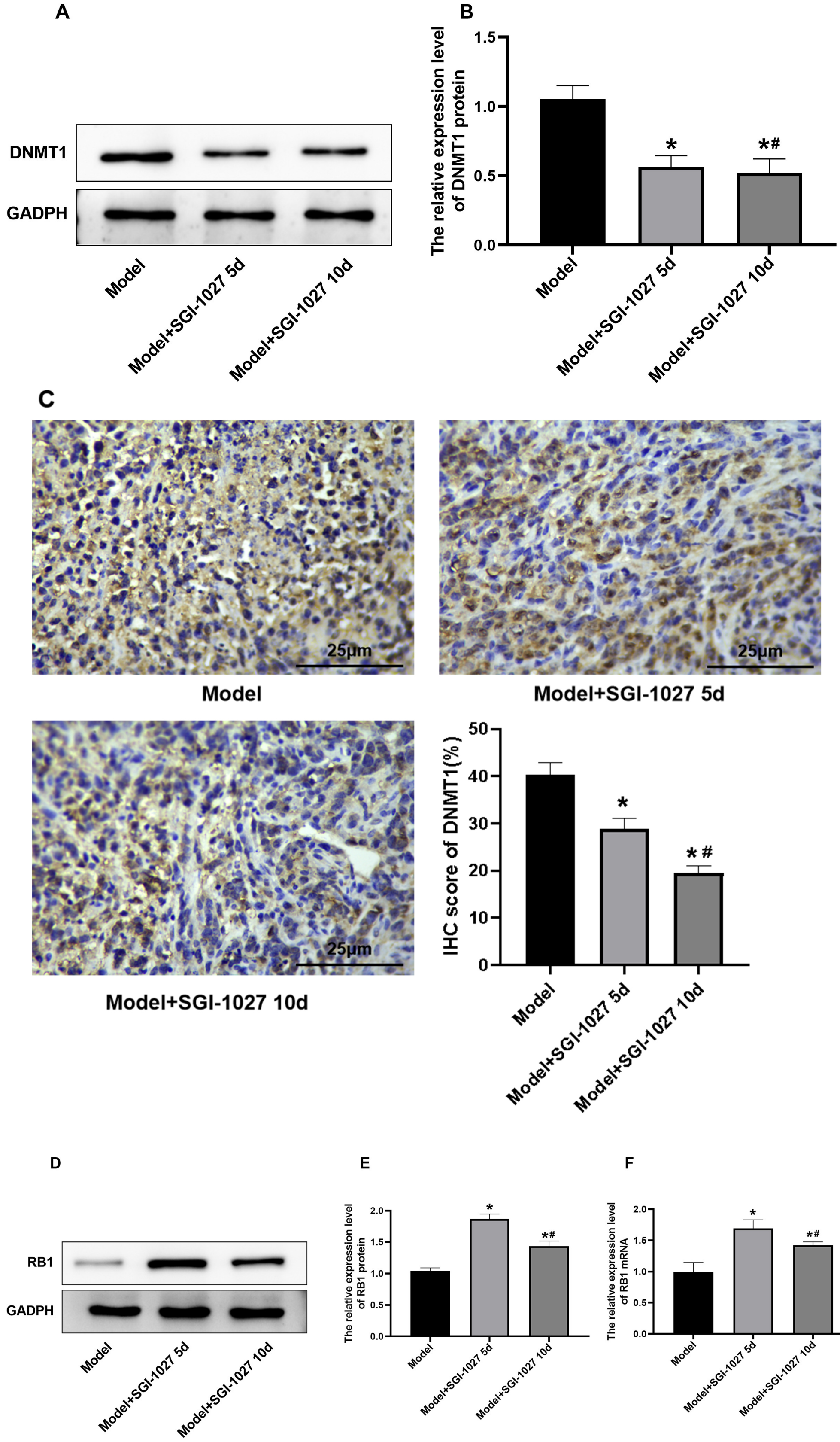

Fig. 6. Effect of SGI-1027 on expression of DNMT1 and RB1 in mice. (A,B) DNMT1 expression was measured by WB (n = 3). (C) DNMT1 expression was determined by immunohistochemistry, the positive areas appear brown to dark brown (n = 3). (D–F) The expression level of RB1 was detected by WB and qRT-PCR (n = 3). **p* < 0.05 versus the Model group, #*p* < 0.05 versus the Model+SGI-1027 5d 15 μmol/L SGI-1027 group. WB, Western blot.

The Impact of SGI-1027 on DNMT1 Activity and RB1 Gene Expression Level in GC Tissue

The experimental results reveal that, in comparison to the Model group, the expression level of DNMT1 in the Model+SGI-1027 5d group and Model+SGI-1027 10d group significantly decreased. The positive rate of DNMT1 also witnessed a substantial decrease, while the expression level of the RB1 increased ($p < 0.05$). Moreover, when compared with the Model+SGI-1027 5d group, there was no significant difference in the expression level of DNMT1 detected by Western blot (WB) in the Model+SGI-1027 10d group, but there were significant differences in other groups ($p < 0.05$) (Fig. 6A–F).

Discussion

GC, a prevalent malignant tumor, typically originates in the gastric mucosal layer or adjacent areas of the stomach. Untreated, it has the potential to metastasize to other organs, posing a significant threat to life [35,36]. The incidence of GC tends to rise with age, particularly in individuals aged 60 and older. Several risk factors contribute to the likelihood of developing GC, including dietary habits, lifestyle, high consumption of salted, pickled, and hot foods, as well as inadequate intake of vegetables and fruits. These factors are considered to be associated with the risk of GC [37,38].

Bacterial infections, particularly Helicobacter pylori infection, may also influence the onset of GC. Individuals infected with H. pylori are more susceptible to GC [39,40]. Additionally, genetic factors play a crucial role, as a family history of GC, especially among first-degree relatives, increases an individual's risk of developing GC [41]. Therefore, recognizing the risk factors for GC and making efforts to avoid these factors are of paramount importance for the prevention and early detection of GC.

Genes are specific regions within the DNA molecule that carry encoded genetic information, determining an organism's hereditary traits and biological functions [42]. Each gene encodes a particular protein or RNA molecule, which performs various functions within cells, such as enzymatic activity, structural support, and signal transduction [43]. Genes exert control over these proteins or RNA through the regulation of their synthesis and function, playing a critical role in the regulation of cell growth, differentiation, and activity [44,45].

Gene expression refers to the process in which the information within DNA is transcribed into RNA and subsequently translated into proteins. The regulation of gene expression is a crucial aspect of an organism's ability to adapt to its environment and maintain normal physiological functions [46,47]. Changes in genes can impact their expression levels, leading to either overexpression or downexpression of certain proteins.

The *RB1* gene plays a crucial normal role in cells as a tumor suppressor, contributing to the orderly progression of the cell cycle [48]. Under normal conditions, the RB1 protein can form complexes with cell cycle proteins D1 and E1, thereby halting further progression of the cell cycle. This means that, under normal circumstances, the RB1 protein regulates cell growth and division, maintaining tissue health and stability.

However, when the *RB1* gene becomes hypermethylated, RB1 protein expression is suppressed, preventing it from adequately inhibiting the cell cycle. This results in the loss of control over the cell cycle, leading to rapid and uncontrolled proliferation. In GC, the overexpression of DNMT1 causes abnormal expression of the *RB1* gene, inhibiting the normal expression of the RB1 protein. This leads to GC cells losing control over the cell cycle, proliferating rapidly, ultimately forming tumors.

In addition to cell cycle regulation, the RB1 protein also plays a vital role in the apoptosis process. Under normal circumstances, the normal function of the RB1 protein helps maintain the apoptosis mechanism of cells, ensuring the timely removal of abnormal or damaged cells. However, when abnormal expression of the *RB1* gene results in impaired function of the RB1 protein, uncontrolled cell cycling prevents cells from entering apoptosis. This may inhibit the apoptotic signaling pathway, resulting in decreased expression of apoptosis-inducing factors like BAX. Meanwhile, BCL-2 typically functions to suppress apoptosis, causing its expression to increase, further promoting the survival and proliferation of GC cells. Therefore, the interaction between the *RB1* gene and DNMT1 plays a pivotal role in the development of GC, influencing cell cycle and apoptosis regulation, ultimately driving the growth and transformation of cancer cells.

SGI-1027, a drug previously studied for its inhibitory effects on DNMT (DNA methyltransferase) activity in liver cancer, has demonstrated efficacy in liver cancer treatment mechanisms [49]. However, its effects in the context of gastric cancer (GC) research have not been extensively explored. The objective of our study was to investigate how SGI-1027 regulates DNMT1 activity in gastric cancer, its impact on *RB1* gene expression, and its effects on the growth and metastasis of gastric cancer cells.

Our research findings indicate that in GC cells, DNMT1 expression was significantly elevated compared to normal gastric epithelial mucosal cells, while *RB1* expression markedly decreased. To explore the impact of SGI-1027 on the expression of DNMT1 and *RB1*, as well as the behavior of GC cells, including cell cycle proteins and apoptosis proteins, we co-cultured different concentrations (15, 20, 25 µmol/L) of SGI-1027 with the GC cell line MKN45 and compared it to untreated MKN45 cells.

Experimental results suggest that treatment with SGI-1027 led to a decrease in DNMT1 expression and an increase in *RB1* expression. Furthermore, SGI-1027 treatment significantly reduced the proliferation, migration, and invasion capabilities of GC cells. Additionally, SGI-1027 treatment results in the downregulation of cell cycle proteins (Cyclin D1, Cyclin E1) and apoptosis proteins (BCL-2) in GC cells, with an increase in the apoptosis-promoting protein BAX. The 25 μmol/L concentration of SGI-1027 shows the most significant changes.

In vivo experimental results demonstrate that compared with the model group, the co-cultured group with SGI-1027 exhibited obvious inhibitory effects after 5 and 10 days. This indicates a significant slowdown in the tumor growth of nude mice and a reduction in lung tumor metastasis.

HE staining revealed that the number of tumor cells in the Model+SGI-1027+5d and 10d groups decreased, and the degree of necrosis was significantly reduced. The activity and positive activity of DNMT1 in tumor tissues significantly decreased, and the expression level of *RB1* increased. This suggests that SGI-1027 may inhibit tumor growth and metastasis by modulating DNMT1 and *RB1*. Notably, the Model+SGI-1027+5d group exhibited the smallest degree of lung metastasis in both treatment durations, indicating the most significant therapeutic effect. This could be attributed to the weakening of the inhibitory effect of MKN45 cells on SGI-1027 after 5 days of culture, leading to the emergence of drug resistance. In contrast, the Model+SGI-1027 group cultured after 10 days showed a decrease in therapeutic effectiveness, possibly due to prolonged exposure to SGI-1027 causing MKN45 cells to develop resistance, diminishing the therapeutic effect. These results suggest the potential therapeutic effect of SGI-1027 in inhibiting tumor growth and reducing lung metastasis. However, further research is needed to gain insight into its therapeutic effects and possible resistance mechanisms at different time points, providing more comprehensive information for future clinical applications.

Conclusions

SGI-1027 inhibits the activity of DNA methyltransferase 1 (DNMT1), effectively promoting the expression of the *RB1* gene. This significantly decelerates the proliferation, migration, and invasion of gastric cancer cells. Simultaneously, it induces apoptosis, suppressing tumor growth and metastasis, thereby offering a potential therapeutic avenue to ameliorate the progression of gastric cancer.

Availability of Data and Materials

The data used and/or analyzed during the current study are available from the corresponding author.

Author Contributions

PG contributed equally to the conception and design of the research study, acquisition of data, analysis and interpretation of the data, and drafting of the manuscript. WH provided technical support in the acquisition of data, performed statistical analysis, and critically revised the manuscript for important intellectual content. WL provided guidance on the design of the research study, contributed to the interpretation of the data, and critically revised the manuscript for important intellectual content. PS provided expertise in the field of study, contributed to the interpretation of the data, and critically revised the manuscript for important intellectual content. All authors have read and approved the final manuscript, and have participated sufficiently in the work to take public responsibility for appropriate portions of the content. All authors agreed to be accountable for all aspects of the work in ensuring that questions related to the accuracy or integrity of any part of the work are appropriately investigated and resolved.

Ethics Approval and Consent to Participate

All animal trials adhere to the “Laboratory Animal Care and Use Guidelines” and obtained the approval of the Ethics Committee of Affiliated Hospital of Nanjing University of Chinese Medicine (202104008).

Acknowledgment

We would like to express our gratitude to the participants who generously gave their time and effort to make this study possible.

Funding

This research received no external funding.

Conflict of Interest

The authors declare no conflict of interest.

References

[1] Joshi SS, Badgwell BD. Current treatment and recent progress in gastric cancer. CA: A Cancer Journal for Clinicians. 2021; 71: 264–279.
[2] Waldum H, Fossmark R. Gastritis, Gastric Polyps and Gastric Cancer. International Journal of Molecular Sciences. 2021; 22: 6548.
[3] Röcken C. Predictive biomarkers in gastric cancer. Journal of Cancer Research and Clinical Oncology. 2023; 149: 467–481.
[4] Onoyama T, Ishikawa S, Isomoto H. Gastric cancer and genomics: review of literature. Journal of Gastroenterology. 2022; 57: 505–516.
[5] Guan WL, He Y, Xu RH. Gastric cancer treatment: recent progress and future perspectives. Journal of Hematology & Oncology. 2023; 16: 57.
[6] Wen L, Cheng F, Zhou Y, Yin C. MiR-26a enhances the sensitivity of gastric cancer cells to cisplatin by targeting NRAS and E2F2. Saudi Journal of Gastroenterology: Official Journal of the Saudi Gastroenterology Association. 2015; 21: 313–319.
[7] Wei S, Sun T, Du J, Zhang B, Xiang D, Li W. Xanthohu-

mol, a prenylated flavonoid from Hops, exerts anticancer effects against gastric cancer *in vitro*. Oncology Reports. 2018; 40: 3213–3222.
[8] Hu S, Molina L, Tao J, Liu S, Hassan M, Singh S, *et al.* NOTCH-YAP1/TEAD-DNMT1 Axis Drives Hepatocyte Reprogramming Into Intrahepatic Cholangiocarcinoma. Gastroenterology. 2022; 163: 449–465.
[9] Wu C, Liu Y, Liu W, Zou T, Lu S, Zhu C, *et al.* NNMT-DNMT1 Axis is Essential for Maintaining Cancer Cell Sensitivity to Oxidative Phosphorylation Inhibition. Advanced Science (Weinheim, Baden-Wurttemberg, Germany). 2022; 10: e2202642.
[10] Geng X, Zhao J, Huang J, Li S, Chu W, Wang WS, *et al.* lnc-MAP3K13-7:1 Inhibits Ovarian GC Proliferation in PCOS via DNMT1 Downregulation-Mediated CDKN1A Promoter Hypomethylation. Molecular Therapy: the Journal of the American Society of Gene Therapy. 2021; 29: 1279–1293.
[11] Jiang Y, Chang YD, Wang M, Sun YP, Bi YJ, Wang ZB, *et al.* Exploring the molecular mechanism of Radix Astragali on colon cancer based on integrated pharmacology and molecular docking technique. World Journal of Traditional Chinese Medicine. 2022; 8: 502–508.
[12] Ren W, Fan H, Grimm SA, Kim JJ, Li L, Guo Y, *et al.* DNMT1 reads heterochromatic H4K20me3 to reinforce LINE-1 DNA methylation. Nature Communications. 2021; 12: 2490.
[13] Esposito CL, Autiero I, Sandomenico A, Li H, Bassal MA, Ibba ML, *et al.* Targeted systematic evolution of an RNA platform neutralizing DNMT1 function and controlling DNA methylation. Nature Communications. 2023; 14: 99.
[14] He Y, Dan Y, Gao X, Huang L, Lv H, Chen J. DNMT1-mediated lncRNA MEG3 methylation accelerates endothelial-mesenchymal transition in diabetic retinopathy through the PI3K/Akt/mTOR signaling pathway. American Journal of Physiology. Endocrinology and Metabolism. 2021; 320: E598–E608.
[15] Zhu X, Lv L, Wang M, Fan C, Lu X, Jin M, *et al.* DNMT1 facilitates growth of breast cancer by inducing MEG3 hypermethylation. Cancer Cell International. 2022; 22: 56.
[16] Liu H, Song Y, Qiu H, Liu Y, Luo K, Yi Y, *et al.* Downregulation of FOXO3a by DNMT1 promotes breast cancer stem cell properties and tumorigenesis. Cell Death and Differentiation. 2020; 27: 966–983.
[17] Gao Y, Luo X, Meng T, Zhu M, Tian M, Lu X. DNMT1 protein promotes retinoblastoma proliferation by silencing MEG3 gene. Nan Fang Yi Ke Da Xue Xue Bao. 2020; 40: 1239–1245. (In Chinese)
[18] Cao X, Liu L, Cao X, Cui Y, Zou C, Chen A, *et al.* The DNMT1/miR-34a/FOXM1 Axis Contributes to Stemness of Liver Cancer Cells. Journal of Oncology. 2020; 2020: 8978930.
[19] Pan T, Ding H, Jin L, Zhang S, Wu D, Pan W, *et al.* DNMT1-mediated demethylation of lncRNA MEG3 promoter suppressed breast cancer progression by repressing Notch1 signaling pathway. Cell Cycle (Georgetown, Tex.). 2022; 21: 2323–2337.
[20] İnce O, Yıldız H, Kisbet T, Ertürk ŞM, Önder H. Classification of retinoblastoma-1 gene mutation with machine learning-based models in bladder cancer. Heliyon. 2022; 8: e09311.
[21] Yang X, Sun H, Tang T, Zhang W, Li Y. Netrin-1 promotes retinoblastoma-associated angiogenesis. Annals of Translational Medicine. 2021; 9: 1683.
[22] Urbschat S, Breitfelder G, Henia M, Schulz-Schaeffer W, Sippl C, Oertel J, *et al.* RB1 promoter methylation in glioblastoma: A rare event in glioblastoma. Oncology Reports. 2023; 50: 143.
[23] Creytens D, Folpe AL, Koelsche C, Mentzel T, Ferdinande L, van Gorp JM, *et al.* Myxoid pleomorphic liposarcoma-a clinicopathologic, immunohistochemical, molecular genetic and epigenetic study of 12 cases, suggesting a possible relationship with conventional pleomorphic liposarcoma. Modern Pathology: an Official Journal of the United States and Canadian Academy of Pathology, Inc. 2021; 34: 2043–2049.
[24] Roohollahi K, de Jong Y, van Mil SE, Fabius AWM, Moll AC, Dorsman JC. High-Level *MYCN*-Amplified *RB1*-Proficient Retinoblastoma Tumors Retain Distinct Molecular Signatures. Ophthalmology Science. 2022; 2: 100188.
[25] Tang H, Long Q, Zhuang K, Han K, Zhang X, Guo H, *et al.* Retinoblastoma tumor suppressor gene 1 enhances 5-Fluorouracil chemosensitivity through SDF-1/CXCR4 axis by regulating autophagy in gastric cancer. Pathology - Research and Practice. 2021; 224: 153532.
[26] Dyson NJ. RB1: a prototype tumor suppressor and an enigma. Genes & Development. 2016; 30: 1492–1502.
[27] Wu Q, Ba-Alawi W, Deblois G, Cruickshank J, Duan S, Lima-Fernandes E, *et al.* GLUT1 inhibition blocks growth of RB1-positive triple negative breast cancer. Nature Communications. 2020; 11: 4205.
[28] Cruz-Gálvez CC, Ordaz-Favila JC, Villar-Calvo VM, Cancino-Marentes ME, Bosch-Canto V. Retinoblastoma: Review and new insights. Frontiers in Oncology. 2022; 12: 963780.
[29] Tu J, Huo Z, Yu Y, Zhu D, Xu A, Huang MF, *et al.* Hereditary retinoblastoma iPSC model reveals aberrant spliceosome function driving bone malignancies. Proceedings of the National Academy of Sciences of the United States of America. 2022; 119: e2117857119.
[30] Plousiou M, De Vita A, Miserocchi G, Bandini E, Vannini I, Melloni M, *et al.* Growth Inhibition of Retinoblastoma Cell Line by Exosome-Mediated Transfer of miR-142-3p. Cancer Management and Research. 2022; 14: 2119–2131.
[31] Wu C, Peng S, Pilié PG, Geng C, Park S, Manyam GC, *et al.* PARP and CDK4/6 Inhibitor Combination Therapy Induces Apoptosis and Suppresses Neuroendocrine Differentiation in Prostate Cancer. Molecular Cancer Therapeutics. 2021; 20: 1680–1691.
[32] Wang ME, Chen J, Lu Y, Bawcom AR, Wu J, Ou J, *et al.* RB1-deficient prostate tumor growth and metastasis are vulnerable to ferroptosis induction via the E2F/ACSL4 axis. The Journal of Clinical Investigation. 2023; 133: e166647.
[33] Gao Q, Chen F, Zhang L, Wei A, Wang Y, Wu Z, *et al.* Inhibition of DNA methyltransferase aberrations reinstates antioxidant aging suppressors and ameliorates renal aging. Aging Cell. 2022; 21: e13526.
[34] Yazici H, Wu HC, Tigli H, Yilmaz EZ, Kebudi R, Santella RM. High levels of global genome methylation in patients with retinoblastoma. Oncology Letters. 2020; 20: 715–723.
[35] Wu H, Fu M, Liu J, Chong W, Fang Z, Du F, *et al.* The role and application of small extracellular vesicles in gastric cancer. Molecular Cancer. 2021; 20: 71.
[36] Bouras E, Tsilidis KK, Triggi M, Siargkas A, Chourdakis M, Haidich AB. Diet and Risk of Gastric Cancer: An Umbrella Review. Nutrients. 2022; 14: 1764.
[37] Wu X, Chen L, Cheng J, Qian J, Fang Z, Wu J. Effect of Dietary Salt Intake on Risk of Gastric Cancer: A Systematic Review and Meta-Analysis of Case-Control Studies. Nutrients. 2022; 14: 4260.
[38] Alipour M. Molecular Mechanism of Helicobacter pylori-Induced Gastric Cancer. Journal of Gastrointestinal Cancer. 2021; 52: 23–30.
[39] Ito M, Tanaka S, Chayama K. Characteristics and Early Diagnosis of Gastric Cancer Discovered after *Helicobacter pylori* Eradication. Gut and Liver. 2021; 15: 338–345.
[40] Sekiguchi M, Oda I, Matsuda T, Saito Y. Epidemiological Trends and Future Perspectives of Gastric Cancer in Eastern Asia. Digestion. 2022; 103: 22–28.
[41] Mattei AL, Bailly N, Meissner A. DNA methylation: a historical perspective. Trends in Genetics: TIG. 2022; 38: 676–707.
[42] Liu M, Yao B, Gui T, Guo C, Wu X, Li J, *et al.* PRMT5-

dependent transcriptional repression of c-Myc target genes promotes gastric cancer progression. Theranostics. 2020; 10: 4437–4452.

[43] Dai X, Ren T, Zhang Y, Nan N. Methylation multiplicity and its clinical values in cancer. Expert Reviews in Molecular Medicine. 2021; 23: e2.

[44] Wei A, Gao Q, Chen F, Zhu X, Chen X, Zhang L, *et al*. Inhibition of DNA methylation de-represses peroxisome proliferator-activated receptor-γ and attenuates pulmonary fibrosis. British Journal of Pharmacology. 2022; 179: 1304–1318.

[45] Liu Y, Cheng H, Cheng C, Zheng F, Zhao Z, Chen Q, *et al*. ZNF191 alters DNA methylation and activates the PI3K-AKT pathway in hepatoma cells via transcriptional regulation of DNMT1. Cancer Medicine. 2022; 11: 1269–1280.

[46] Lee J, Song JH, Park JH, Chung MY, Lee SH, Jeon SB, *et al*. Dnmt1/Tet2-mediated changes in Cmip methylation regulate the development of nonalcoholic fatty liver disease by controlling the Gbp2-Pparγ-CD36 axis. Experimental & Molecular Medicine. 2023; 55: 143–157.

[47] Beird HC, Wu CC, Nakazawa M, Ingram D, Daniele JR, Lazcano R, *et al*. Complete loss of *TP53* and *RB1* is associated with complex genome and low immune infiltrate in pleomorphic rhabdomyosarcoma. HGG Advances. 2023; 4: 100224.

[48] Zhang Y, Zhang H, Li X. MicroRNA-215 promoted the progression of nasopharyngeal carcinoma through targeting RB1 and activating Wnt/β-catenin pathway. Journal of B.U.ON.: Official Journal of the Balkan Union of Oncology. 2020; 25: 1579–1586.

[49] Sun N, Zhang J, Zhang C, Zhao B, Jiao A. DNMTs inhibitor SGI-1027 induces apoptosis in Huh7 human hepatocellular carcinoma cells. Oncology Letters. 2018; 16: 5799–5806.